Title

A soil matrix capacity index to predict mineral-associated but not particulate organic carbon across a range of climate and soil pH

Authors

Alison E. King[1*], Joseph P. Amsili[2], S. Carolina Córdova[3], Steve Culman[4], Steven J. Fonte[1], James Kotcon[5], Mark Liebig[6], Michael D. Masters[7], Kent McVay[8], Daniel C. Olk[9], Meagan Schipanski[1], Sharon K. Schneider[10], Catherine E. Stewart[11], M. Francesca Cotrufo[1]

[1] Department of Soil and Crop Sciences, Colorado State University, Fort Collins, CO, USA

[2] School of Integrative Plant Science, Cornell University, Ithaca, NY, USA

[3] W. K. Kellogg Biological Station, Michigan State University, Hickory Corners, MI, USA

[4] Department of Crop and Soil Sciences, Washington State University, Pullman, WA, USA

[5] Division of Plant and Soil Sciences, West Virginia University, Morgantown, WV, USA

[6] Northern Great Plains Research Laboratory, USDA-ARS, Mandan, ND, USDA

[7] Institute for Sustainability, Energy, and Environment, University of Illinois, Urbana, IL, USA

[8] Southern Agricultural Research Center, Montana State University, Bozeman, MT, USA

[9] National Laboratory of Agriculture and the Environment, USDA-ARS, Ames, IA, USA

[10] USDA, Agricultural Research Service, North Central Agricultural Research Laboratory, Brookings, SD, USA

[11] Plains Area Center for Agricultural Resources Research, USDA-ARS, Fort Collins, CO, USA

***Corresponding Author:** Alison E. King, alison.elinor.king@colostate.edu, https://orcid.org/0000-0002-4155-577X

Keywords

soil organic matter, carbon, size fractionation, physicochemical properties, particulate organic carbon, mineral-associated organic carbon

Abstract

Understanding controls on soil organic carbon (SOC) will be crucial to managing soils for climate change mitigation and food security. Climate exerts an overarching influence on SOC, affecting both carbon (C) inputs to soil and soil physicochemical properties participating in C retention. To test our hypothesis that climate, C inputs,

and soil properties would differently affect particulate organic carbon (POC) and mineral-associated organic carbon (MAOC), we sampled 16 agricultural sites (n = 124 plots) in the United States, ranging in climate (mean annual precipitation (MAP) - potential evapotranspiration (PET; MAP-PET)), soil pH (5.8 – 7.9), and soil texture (silt + clay = 13 – 96%). As MAP-PET increased, soils increased in oxalate-extractable iron (Fe_O) and aluminum (Al_O), decreased in exchangeable calcium (Ca_{ex}) and magnesium (Mg_{ex}), and received greater C inputs. Soil physicochemical properties did not strongly predict POC, confirming the relative independence of this SOC fraction from the soil matrix. In contrast, MAOC was well predicted by combining $Al_O + [1/2]Fe_O$ with $Ca_{ex} + Mg_{ex}$ in a 'matrix capacity index', which performed better than individual soil physicochemical properties across all pH levels ($r > 0.79$). Structural equation modeling indicated a similar total effect of MAP-PET on MAOC and POC, which was mediated by total C inputs and the matrix capacity index for MAOC but not POC. Our results emphasize the need to separately conceptualize controls on MAOC and POC and justify the use of a unified soil matrix capacity index for predicting soil MAOC storage.

Acknowledgments

We gratefully acknowledge the Colorado State University Soil, Water & Plant Testing Laboratory, Cotrufo Soil Innovation Laboratory members, and Jim Ippolito for technical support. Thanks to Matt Liebman and Ilsa Kantola for contributing crop yield data and to Tom Moorman, Michael Thompson, Ala Khaleel, Paul Jasa, Harold van Es, and Michael H. Davis for site access and sampling. Five anonymous reviewers offered feedback that improved the manuscript. Funding for this project was provided by the United States Department of Agriculture National Institute of Food and Agriculture Postdoctoral Fellowship to A. E. King (Award 2020-67034-31762). Soils from Kellogg Biological Station were provided with support from the Great Lakes Bioenergy Research Center, U.S. Department of Energy, Office of Science, Office of Biological and Environmental Research (Award DE-SC0018409), by the National Science Foundation Long-term Ecological Research Program (DEB 1832042) at the Kellogg Biological Station, and by Michigan State University AgBioResearch.

Introduction

Maintaining or increasing soil organic carbon (SOC) in agricultural soils will be crucial for mitigating climate change (Minasny et al. 2017; Lessmann et al. 2022) and for supporting soil functioning (King et al. 2020; Cotrufo and Lavallee 2022). To effectively manage agricultural SOC, we need to develop process-based models of SOC based on a sound understanding of how SOC responds to environmental controls. Although environmental controls on SOC storage have a rich history of theoretical and empirical work, encompassing SOC responses to climate (Jobbagy and Jackson 2000), soil texture (Hassink 1997) and other soil physicochemical properties (Rasmussen et al. 2018; Rowley et al. 2018; Heckman et al. 2020), and carbon (C) inputs (Six et al. 2002), on-going refinements are yet to be fully integrated. For instance, separating SOC into distinct physical fractions is increasingly leveraged to improve our understanding of environmental controls on SOC storage (Cotrufo et al. 2021; Yu et al. 2022). Nevertheless, to our knowledge no studies have synthesized climate, soil physicochemical, and C input controls on agricultural soil C fractions at a continental scale.

Conceptualizing SOC into contrasting fractions of mineral-associated organic carbon (MAOC) and particulate organic carbon (POC) has been proposed to aid in understanding controls on SOC storage (Lavallee et al. 2020). The more stable MAOC pool forms primarily from microbial necromass and soluble, unprocessed plant compounds (Kallenbach et al. 2016; Liang et al. 2017) and is primarily stabilized through adsorption, wherein soil minerals protect adsorbed C from decomposition (Kleber et al. 2015). In contrast, POC is formed predominantly from structural plant inputs and has shorter residence times than MAOC (von Lützow et al. 2007), but may persist through a combination of physical and physiological constraints on decomposers (Cotrufo and Lavallee 2022). Given these contrasting pathways of formation and mechanisms of persistence for POC and MAOC (Lavallee et al. 2020), these fractions may be regulated by different suites of controls from among those factors already widely recognized in controlling SOC.

Climate can be viewed as an overarching control on SOC pools, because it can affect factors that control both C inputs to soil and losses of C from soil (Cotrufo and Lavallee 2022). The control of climate on C inputs operates mainly via water limitations on net primary productivity – and consequently C inputs – at continental scales (Gentine et al. 2019). Water availability can be estimated via water balance as the difference between mean annual precipitation (MAP) and potential evapotranspiration (PET; MAP-PET). In turn, C inputs to soil often (Gulde et al. 2008), but not always (Zhou et al. 2019), increase SOC. To date, it is unclear whether C inputs similarly affect POC and MAOC pools. As POC is minimally dependent on protection from the soil matrix, POC formation may be

88 expected to more directly reflect plant C inputs to soil than MAOC. The formation of MAOC is expected to depend
89 on microbial transformations and soil matrix adsorption capacity (Cotrufo et al. 2013), and may therefore exhibit a
90 moderated relationship to C inputs. Currently, many process-based models predict a saturating increase of SOC with
91 increases in C inputs (Georgiou et al. 2021; Zhang et al. 2021), but these predictions may be refined by assessing the
92 impact of C inputs on contrasting SOC fractions.

93 Climate also controls C losses from the soil, including via microbial activity and soil physicochemical
94 properties. While microbial activity has received abundant attention (Zhang et al. 2008), soil physicochemical
95 properties are increasingly acknowledged for their protective capacity over SOC (Rasmussen et al. 2018). Soil
96 physicochemical properties are modified by MAP-PET: wetness decreases soil pH (Slessarev et al. 2016), increases
97 oxalate-extractable iron and aluminum (Fe_O and Al_O; Hall et al. 2020), and decreases exchangeable calcium (Ca_{ex};
98 von Fromm et al. 2021). As Ca_{ex} and $Al_O + Fe_O$ are stabilizing agents of SOC, they therefore introduce a climate-
99 dependent role of soil physicochemical properties in C retention (Rasmussen et al. 2018; Rowley et al. 2018). The
100 extent to which these soil properties influence retention of POC vs retention of MAOC has been rarely explored
101 empirically, but it might be expected that soil physicochemical properties more closely control MAOC compared to
102 POC given the dependence of MAOC on matrix protection (Kleber et al. 2015). Updating the soil physicochemical
103 controls for different soil fractions is especially likely to improve soil C modeling, because currently soil C models
104 rely on soil texture as the property that controls partitioning of new C inputs to soil (Georgiou et al. 2021; Zhang et
105 al. 2021).

106 A tool that would aid in modeling soil physicochemical controls on MAOC (and potentially on POC)
107 across climates would be a widely applicable, quantitative measure of the capacity of the soil matrix to stabilize C.
108 Rasmussen et al. (2018) showed that soil texture was not a useful predictor of SOC in a global dataset and suggested
109 that stabilization of SOC by soil physicochemical properties is pH- and climate-specific: exchangeable calcium
110 (Ca_{ex}) dominates soil C stabilization in high pH and arid environments, while Fe_O and Al_O dominate in low pH and
111 humid environments. It remains unclear how to advance process-based SOC models with this division, i.e., whether
112 is it necessary to introduce a pH cutoff at which some soil properties affect C stabilization but others do not, or if a
113 synthetic index for the stabilization capacity of the soil matrix could serve universally to inform SOC dynamics
114 across soil pH levels.

To investigate a suite of interacting environmental controls on SOC, POC, and MAOC in agricultural soils, we studied topsoils (0–20 cm) from 16 long-term agricultural research sites and 124 plots across the United States. We selected sites to include soils of the broadest pH range feasible under agriculture – expected to result in a range of soil polyvalent exchangeable cations (Ca_{ex} + Mg_{ex}) and Al_O + Fe_O. We asked: how does climate influence C inputs, soil physicochemical properties, and SOC, POC, and MAOC? As soil physicochemical properties and C inputs are potential drivers of SOC, POC, and MAOC, we aimed to investigate relationships between them independently and to evaluate whether synthesizing soil physicochemical properties could be used to calculate a widely applicable soil matrix capacity index. Finally, we aimed to assess the extent to which effects of MAP-PET on POC and MAOC storage were mediated by C inputs and soil physicochemical properties. We hypothesized, broadly, that POC and MAOC would exhibit distinct responses to environmental controls. Specifically, we hypothesized that C inputs would be a stronger control on POC than on MAOC due to the independence of POC from matrix protection, and that MAOC would be better explained by soil physicochemical properties than POC due to the dependence of MAOC on matrix protection.

Methods

Site selection and soil sampling

Soils were sampled from 0–20 cm in the fall of 2020 from 16 agricultural sites (SI Table 1). From each site, 6–10 plots were sampled, which represented two replicated treatments of contrasting management practices. As our aim was to assess continental-scale relationships, we did not assess soil response to management histories, but used the contrasting management to achieve differences in C inputs within the same climate and soil type. All plots received agronomically realistic rates of synthetic N fertilizer, most were under no-till, and no plots received exogenous organic amendments or irrigation. For complete information on sites, soil sampling, and sample processing, see supplementary information text and SI Tables 1–3.

Soil physicochemical properties

We assessed a suite of soil physicochemical properties on each plot-level soil sample. Soil pH was measured in a slurry of 1:1 soil:water by mass after 10 minutes of rest. Soil texture was assessed using the

hydrometer method to determine clay content and mass recovery of sand particles (> 53 μm) was used to determine sand content. Soil exchangeable cations were extracted in ammonium acetate following Thomas (1982). Briefly, ~2.5-g of 2-mm sieved, air-dry soil was shaken for 30 minutes with 25-mL 1N ammonium acetate at pH 7, then filtered through a Whatman #1 filter paper (nominal pore size = 11 μm) and analyzed via inductively coupled plasma optical emission spectrometer (ICP-OES, Optima 7300 DV, PerkinElmer, Waltham, MA, USA) for Ca^{2+} and Mg^{2+}, reported by total positive charge (cmol kg $soil^{-1}$). These polyvalent cations provide mechanism of C retention via their role in cation bridging (Wiesmeier et al. 2019). Soil Fe and Al were extracted via the acid ammonium oxalate method following Loeppert and Inskeep (1996). This method estimates Fe and Al in amorphous phases (referred to as Fe_O and Al_O). For the acid ammonium oxalate extraction, ~0.5-g ground, air-dry soil was mixed with 30-mL 0.175 mol/L ammonium oxalate at pH 3 and shaken for 2 hours in the dark, then filtered through a Whatman #1 filter paper. Calcareous soils were identified by reaction with HCl, as described below, and their carbonates removed before the acid ammonium oxalate extraction by reacting the sample with 30-mL 1 mol/L ammonium acetate at pH 5.5. Ammonium oxalate extracts were also run on the ICP-OES, and summation of Al_O and Fe_O was corrected to larger atomic mass of Fe by dividing Fe by half ([1/2]Fe_O, Wagai et al. 2020). All analyses performed were air-dry soils and are reported in oven-dry equivalents.

Soil size fractionation into POC and MAOC

Soils were separated by size into sand + POC (> 53 μm) and silt + clay + MAOC (<53 μm) following Cambardella and Elliott, (1992). These fractions are hereafter referred to as 'POC' and 'MAOC', respectively. Briefly, 5.75–6.25-g of 2-mm sieved bulk soil dried at 60° C was shaken for 18 hours with 12 glass beads in 30-mL 0.5% sodium hexametaphosphate to disrupt all aggregates. The resulting soil slurry was rinsed with DI water over a 53 μm sieve to isolate POC and remove glass beads. Soil solution passing through the sieve was deemed MAOC. Both the POC and MAOC fractions were dried at 60° C until reaching constant mass. Recoveries of the initial soil masses in the summed fractions were between 95 and 103% for all samples, with a mean recovery of 100.5%. Soils and fractions containing carbonates (identified by effervescence after addition of 5% HCl, 18 samples) were treated to remove inorganic carbon via HCl fumigation (Harris et al. 2001). SOC, MAOC, and POC were ground using a mortar and pestle before running on a Costech elemental analyzer (Costech ECS4010, Analytical Technologies, Inc., Milano, Italy). The average recovery of SOC in POC and MAOC fractions was 92% (standard error = 0.9%).

Crop C inputs to soil and climate data

The best available crop yield data from across the history of each site were used to estimate C inputs from crops to soil (SI Table 4). Allometric equations (Bolinder et al. 2007) were used to estimate shoot and root + exudate inputs for each crop; belowground inputs were truncated to the 20–cm soil depth sampled using crop-specific root distributions (Fan et al. 2016). For perennial crops grown over multiple years, annual root inputs were estimated as 62% of root inputs from the initial year, following an assumption of partial root turnover (King and Blesh 2018). Shoot inputs were reduced by the proportions of shoots that were removed for stover production, if any, and rotation-average crop inputs were calculated (Mg C ha^{-1} yr^{-1}). As yield information was not consistently available for all harvests across site history, we did not investigate interannual variability in C inputs. For each site, mean annual precipitation (MAP) and mean annual air temperature (MAT) were extracted from WorldClim at 30 s resolution (Fick and Hijmans 2017, 1970–2000). Potential evapotranspiration (PET), calculated using a Penman-Montieth equation, was extracted from the Global Aridity Index Database v2 (Trabucco and Zomer 2018, 1970–2000), and was used to estimate ecosystem water balance (MAP-PET; Slessarev et al. 2016).

Calculation of soil matrix capacity index

To investigate the capacity for combined values of Al_O + [1/2]Fe_O and Ca_{ex} + Mg_{ex} to stabilize SOC, we calculated a matrix capacity index (MCI) for all 124 plots across the 16 sites. First, to overcome different reporting units for Al_O + [1/2]Fe_O and Ca_{ex} + Mg_{ex} (Rasmussen et al. 2018), we calculated their standardized values for each observation in the sample (n=124) using the z-score approach:

$$Z = \frac{x-u}{\sigma} \quad [1]$$

where Z is the standardized value, x is the observed value, u is the mean of the sample and σ is the standard deviation of the sample. The Z-score standardization results in a vector with the same relative distances between all points as the original vector but with a mean of zero and a standard deviation of 1. In our data, means of samples were 2.22 g kg $soil^{-1}$ for Al_O + [1/2]Fe_O and 18.02 cmol kg $soil^{-1}$ for Ca_{ex} + Mg_{ex}, and standard deviations were 0.75 g kg $soil^{-1}$ for Al_O + [1/2]Fe_O and 8.70 cmol kg $soil^{-1}$ for Ca_{ex} + Mg_{ex}. To calculate the reported MCI, we summed standardized values for each observation:

$$MCI = Z_{Ca_{ex}+Mg_{ex}} + Z_{Al_O+[\frac{1}{2}]Fe_O} \quad [2]$$

where $Z_{Ca_{ex}+Mg_{ex}}$ is the standardized value of Ca_{ex} + Mg_{ex} and $Z_{Al_O+[\frac{1}{2}]Fe_O}$ is the standardized value of Al_O + [1/2]Fe_O. Plot-level MCI values were averaged within each site for subsequent analyses, to align with data treatment for all other soil physicochemical properties. Multiple regression using all possible model subsets of Al_O, Fe_O, Ca_{ex}, Mg_{ex} and silt + clay identified Al_O, Fe_O, and Ca_{ex} as the best predictors of MAOC based on adjusted R^2 values (SI Table 5), whereas the same model selection with summed soil physicochemical properties identified Al_O + [1/2]Fe_O and Ca_{ex} + Mg_{ex} as the best predictors (SI Table 6). Thus, model selection did not include Mg in the best model initiated with individual soil properties across these sites. In light of acknowledged soil chemical controls on SOC (Wiesmeier et al. 2019), and considering previous efforts to synthesize soil matrix controls on SOC (Possinger et al. 2021), we retained Mg_{ex} in the proposed MCI in all main figures but also include tests with the MCI as calculated with Al_O + [1/2]Fe_O and Ca_{ex} in SI Tables 8-10.

Statistical methods

We used simple linear regression to test for relationships between soil physicochemical and climatic factors and their relationships with SOC, POC, and MAOC across the entire dataset. We did not use mixed models with a random effect for site, which would have estimated common slopes aggregated from within-site relationships, because the focus of this study was on between-site relationships. In some cases, relationships between predictor and response variables exhibited heteroskedasticity of variance (Bruesch-Pagan test p-value < 0.05). In these cases, we attempted to remove heteroskedasticity by log or square root transforming either predictor or response. Where a data transformation was successful, we applied it to the reported regression coefficients and indicate in every instance where a transformation was used. Where these data transformations did not improve variance distributions, we used raw data in regressions. We used z-score standardized parameters only for the MCI data; no other data were z-score standardized. Low and high soil pH groups were delineated based on the median of the sample (pH = 6.5), with n = 8 for the low pH group and n = 8 for the high pH group.

We used structural equation modeling using the R package '*lavaan',* to investigate the direct and indirect effects of MAP-PET, C inputs, and soil physicochemical properties on POC and MAOC. To construct the structural equation models (SEM), we chose the C input and the soil physicochemical parameters that were most closely related to MAOC or POC based on our linear regressions (Al_O + Fe_O only for POC, as no C input variables were

significant; total C and the MCI for MAOC). Each model allowed for a direct effect of MAP-PET on the SOC fraction as well as indirect pathways for an effect of MAP-PET on SOC via C inputs (MAOC only) and the other via a soil physicochemical property. Despite the relatively low number of observations in our SEMs, the model fit criteria were met: both models had a comparative fit index (CFI) of > 0.9, root mean square error of approximation (RMSEA) of < 0.08, and standardized root mean square residual (SRMR) of < 0.08; (Hooper et al. 2008). We assessed direct and indirect effects of MAP-PET on POC and MAOC by extracting coefficients from individual pathways, then multiplying these coefficients to calculate indirect pathways (e.g., effect of MAP-PET on total C inputs and effect of total C inputs on MAOC); we summed indirect coefficients for both indirect pathways to estimate total indirect effects (SI Tables 12–13). All analyses were carried out in R version 4.1.2.

Results and Discussion

Climate influence on soil physicochemical properties and C inputs, SOC, POC, and MAOC

The sampling sites spanned a climatic gradient in MAP-PET (-1675 to -112 mm, Fig. 1, SI Table 1). Although the study area also encompassed a range of MAT (5.7–12.4 °C) and MAP (357–1066 mm), MAP-PET emerged as a more consistent driver of soil physicochemical properties and C inputs than either MAP or MAT. Compared to MAP-PET, MAP exhibited similar but less defined relationships to soil physicochemical properties and C inputs, while MAT was minimally related to both (SI Table 7). As expected following previous work (Slessarev et al. 2016; von Fromm et al. 2021), MAP-PET was associated with decreasing soil pH and $Ca_{ex} + Mg_{ex}$ and increasing $Al_O + [1/2]Fe_O$ (Fig 1a-b). In our dataset, a particularly high pH site (pH = 7.9) contributed to producing these previously established relationships between soil pH, $Ca_{ex} + Mg_{ex}$ and $Al_O + [1/2]Fe_O$. The observed variability in some relationships, for instance between MAP-PET and $Ca_{ex} + Mg_{ex}$ ($R^2 = 0.23$), likely emerges from soil factors not assessed, such as soil age, which interacts with climate and parent material in creating soil weathering status.

Greater MAP-PET was also associated with increased total C inputs (Fig 1d), which aligns with reduced moisture constraints on plant productivity (Gentine et al. 2019). Variability in total C inputs around the upper range of MAP-PET (Fig 1d) may also reflect a loosening of moisture constraints on plant productivity and introduction of soil or agricultural management influences. In a similar vein, shoot C inputs were less sensitive to MAP-PET than root C inputs (SI Table 7, $R^2 = 0.05$ vs. $R^2 = 0.50$), which was likely due to variable harvesting of aboveground

biomass across these sites. For instance, at some sites, crop aboveground biomass was fully removed (e.g., for hay or biofuel), whereas at other sites all the stem and leaf biomass were returned after grain harvest. Given the relatively consistent return of root inputs to soil, root inputs more closely reflect a moisture constraint on overall crop productivity for agricultural systems. Soil C pools also exhibited positive relationships to MAP-PET (Fig 1e-g); we used SEMs to explore the direct vs. indirect effects of MAP-PET on these soil C pools.

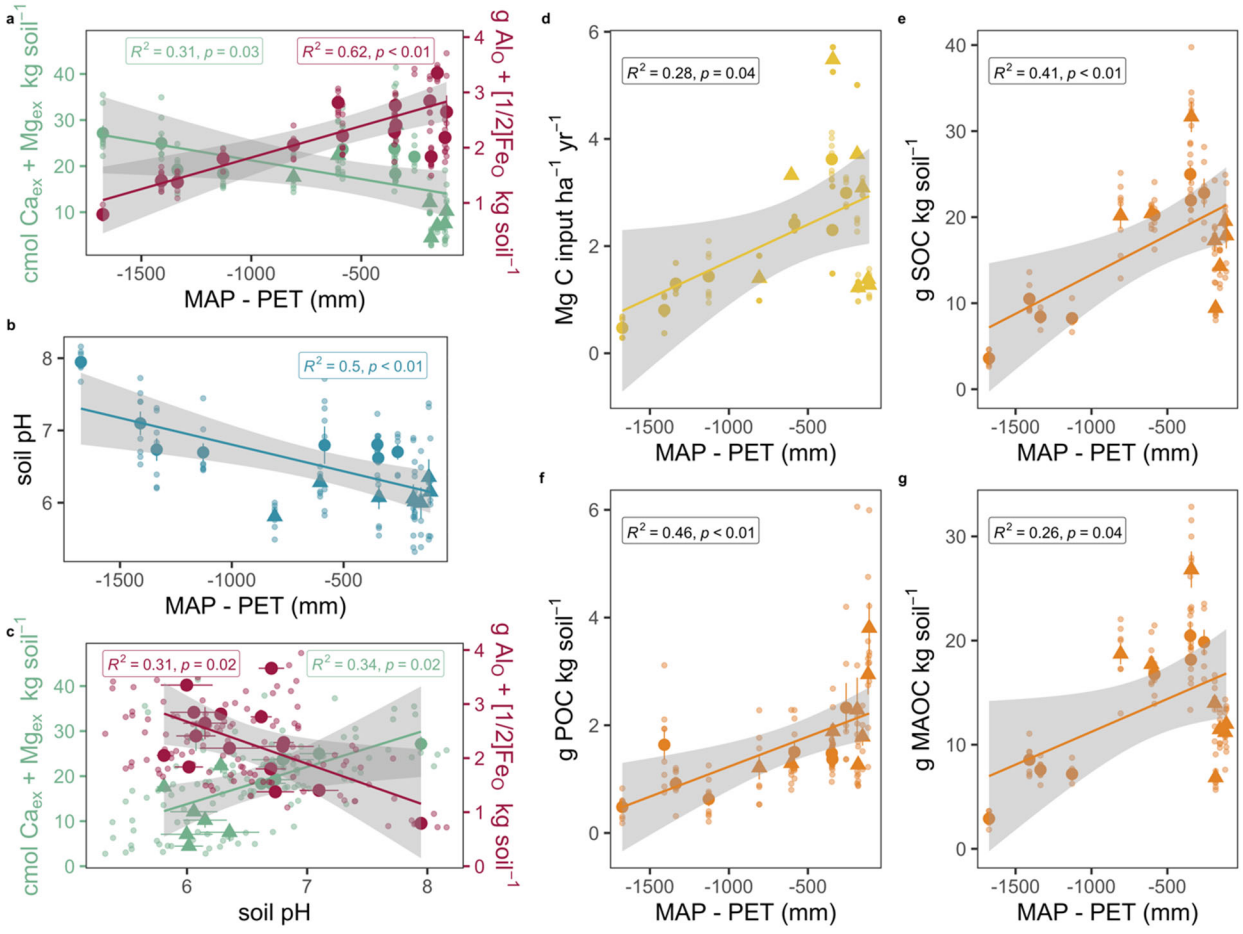

Fig. 1 Relationships between mean annual precipitation minus potential evapotranspiration (MAP-PET), soil pH, and soil physicochemical properties (left panels), and relationships between MAP-PET, carbon (C) inputs, and soil C (right panels). Soils measured 0–20 cm depth across 16 agricultural sites in the United States. Large points represent site-level averages and small points represent plots within sites (n = 124). Large point circles = soil pH > 6.5 large points triangles = soil pH < 6.5. Error bars represent standard errors; standard errors not available for C inputs. Gray bars represent 95% confidence intervals. Axis text colors for panels (a) and (c) correspond to color of

points and regression lines. In panels (d-g), orange points correspond to soil C observations while yellow points correspond to C input observations. Regression coefficients for data shown, with related tests, are reported in SI Table 7.

Effect of soil physicochemical properties and C inputs on SOC, POC, and MAOC

We show that SOC response to soil physicochemical factors is a composite of the responses of various controls that operate distinctly on POC vs MAOC pools (Fig 2). Consistent with our hypothesis, soil physicochemical factors were stronger controls on MAOC than POC. Our finding that MAOC depends on stabilization by reactive surfaces of the soil matrix is supported by previous work (Kleber et al. 2015). We find that Ca_{ex} + Mg_{ex} and Al_O + [1/2]Fe_O better represent these effects on MAOC stabilization than silt + clay. Predictors of total SOC were more similar to those of MAOC than of POC, which was expected as MAOC made up the bulk of SOC (average = 81%), as is common in agricultural soils (Lugato et al. 2021). While there was evidence of a positive association between Al_O + [1/2]Fe_O and increased POC (Fig 2), our finding that POC overall was not as well predicted by soil physicochemical properties as MAOC is mirrored in findings from previous work (Hassink 1997; Six et al. 2002).

When soils were divided into low and high pH groups, soil Ca_{ex}, Mg_{ex}, Al_O, and Fe_O emerged as having stronger association with MAOC in the pH group in which they were less abundant (Fig 3). We observed that Ca_{ex} + Mg_{ex} exhibited much weaker association with MAOC in high pH soils compared to low pH soils, while Al_O + [1/2]Fe_O exhibited weaker associations with MAOC in the low pH soils (Fig 3, SI Table 7). To some extent, this observation may be explained by soil interactions with climate. For instance, some high pH, arid soils containing $CaCO_3$ (which enters into Ca_{ex} during extraction) also supported low C inputs, likely due to a moisture constraint on crop productivity. While we removed inorganic C from these soils prior to analysis, the effect of low C inputs *in situ* may have outweighed any effect of $CaCO_3$ in contributing to aggregate- or mineral-associated C stabilization (Rowley et al. 2021). The lower R^2 of the relationship between Al_O + [1/2]Fe_O and MAOC in the low pH soils in which these compounds are more abundant may be explained by an excess of Al_O + [1/2]Fe_O relative to MAOC, although confirmation of this concept requires further investigation.

Contrary to our hypothesis, C inputs were a better predictor of MAOC than POC, which held when analyzed across shoot, root, and total C inputs (Fig 4). This finding overturned our expectation of matrix-mediated soil C

stabilization contrasting with C input-dependent POC pools. We now propose that C inputs are a poor predictor of POC in agricultural soils because POC pools are more controlled by loss pathways, being less protected (supported by more rapid turnover times, Poeplau et al. 2018) and more vulnerable to the micro-climate effects of decomposition than MAOC. Differences in C input chemistry between sites due to the range of crop species planted, from leguminous annual cover crops to perennial grasses, likely also contributed to differential rates of retention of C inputs (Johnson et al. 2007). While it is surprising that root inputs in particular were poorly associated with an overall increase in POC given their preferential retention in soil (Austin et al. 2017), an increase in minimum values of POC with root inputs does support the current understanding of the role of root inputs for SOC. Total C and shoot C inputs best predicted MAOC levels, and we explore interrelationships between C inputs and MAOC through the use of SEM below.

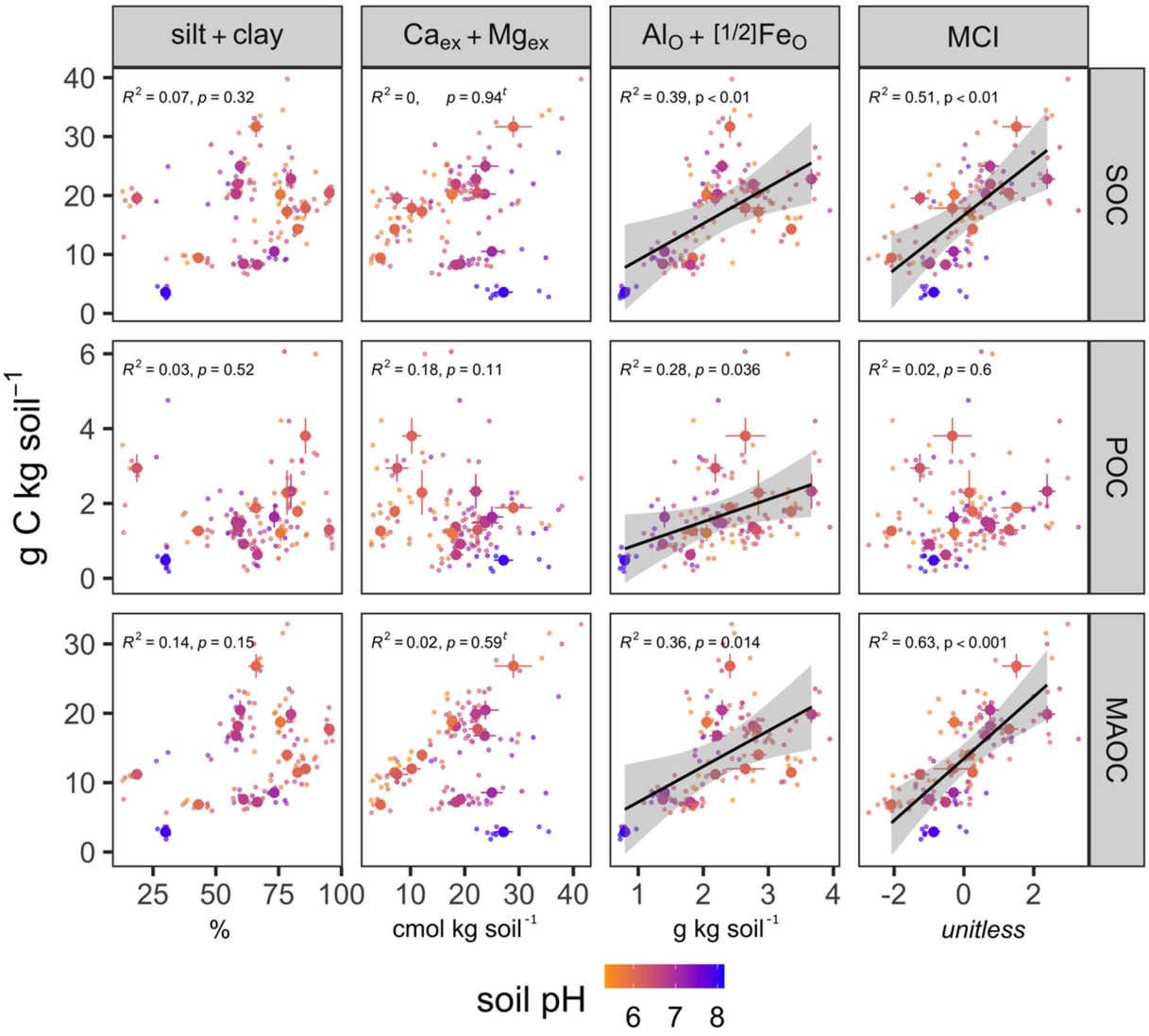

307

308 **Fig. 2** Effect of soil physicochemical properties on soil organic carbon (SOC), particulate organic carbon (POC),
309 and mineral-associated organic carbon (MAOC), 0–20 cm depth, across 16 agricultural sites (n = 124 plots) in the
310 United States. Large points represent site-level averages and small points represent plots within sites (n = 124).
311 Error bars represent standard errors. Regression lines plotted when $p < 0.05$. A '*t*' indicates the p-value and R^2
312 reflect response variables that were log-transformed to reduce heteroskedasticity. $Ca_{ex} + Mg_{ex}$ = sum of
313 exchangeable Ca and Mg. $Al_O + [1/2]Fe_O$ = sum of oxalate-extractable Al and oxalate-extractable Fe. MCI = matrix
314 capacity index, defined in Methods. Complete regression coefficients for all observations and separate pH groups,
315 and with Ca_{ex}, Mg_{ex}, Fe_O, and Al_O separated, are reported in SI Tables 8–10.

316

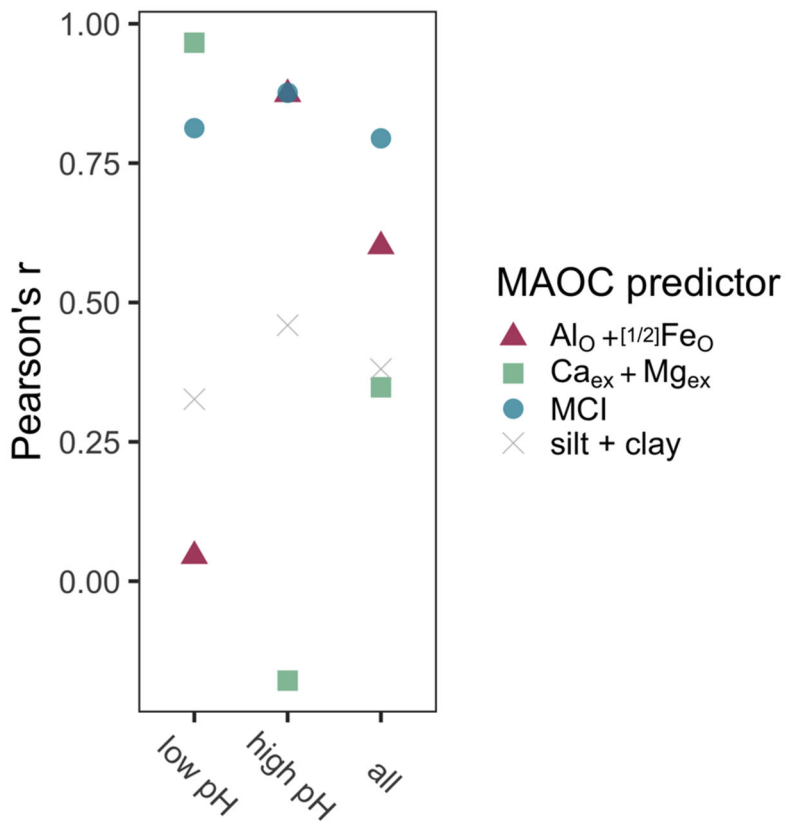

317

318 **Fig. 3** Pearson correlation coefficients between soil physicochemical properties and soil mineral-associated organic

319 carbon (MAOC), 0–20 cm depth, across 16 agricultural sites (averaged from 124 plots) in the United States. Site-

320 level average soil pH ranged from 5.8–6.4 in the low pH group and 6.6–7.9 in the high pH group. MCI = matrix

321 capacity index, the sum of z-score standardized values of Ca_{ex} + Mg_{ex} and Al_O + [1/2]Fe_O, defined in Methods.

322

323

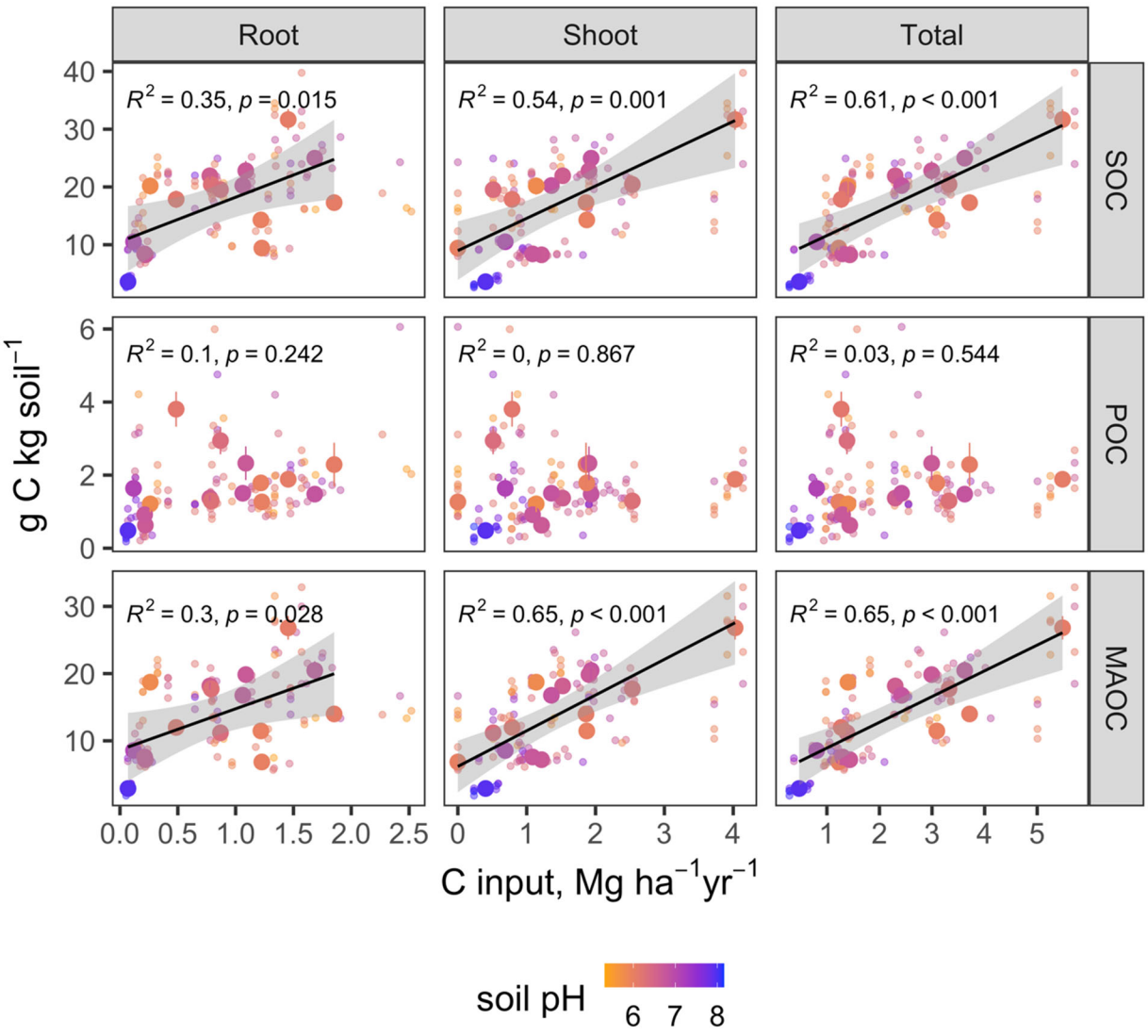

Fig. 4 Relationships between root, shoot, and total average C inputs and soil organic carbon (SOC), particulate organic carbon (POC), and mineral-associated organic carbon (MAOC), 0–20 cm depth, across 16 agricultural sites (n = 124 plots) in the United States. Large points represent site-level averages and small points represent plots within sites (n = 124). Regression lines plotted when p < 0.05. Error bars represent standard errors; standard errors not available for C inputs. Complete regression coefficients for all observations are reported in SI Table 11.

A unified index for soil matrix capacity to stabilize MAOC

Our approach of creating an MCI to predict MAOC, based on the unified stabilization capacity of Ca_{ex} + Mg_{ex} with Fe_O and Al_O, appears justified, as the MCI had more predictive power over MAOC than other physicochemical properties (Fig 2, Fig 3; SI Tables 5–6). The MCI also predicted MAOC when calculated with only Ca_{ex} as the exchangeable cation (SI Table 10), likely due to greater abundance of Ca_{ex} compared to Mg_{ex} in our soils. Further investigation is needed to determine if Mg_{ex} is required in an MCI than spans a broader range of climate and vegetation covers. Mechanisms of Ca_{ex}, Mg_{ex}, Fe_O and Al_O in stabilizing soil C, which have been proposed and examined elsewhere, include cation bridging and ligand exchange with organic complexes, as well as aggregate formation (Rowley et al. 2018; Wagai et al. 2020).

The pH-independent MCI proposed here (Fig 2, Fig 3) appears at first to contrast findings of Rasmussen et al. (2018). Rasmussen et al. (2018) showed that soil physicochemical properties associated with SOC differ in arid vs. humid climates, i.e., Fe_O and Al_O were positively related to SOC in humid climates and Ca_{ex} was positively related to SOC in arid climates, with only a moderate degree of overlap. Rasmussen et al. (2018) attributed these patterns to a differential abundance of Fe_O, Al_O, and Ca_{ex} with changes in water balance and soil pH. The same patterns of differential abundance of these compounds across soil pH are evident in this study (Fig 1 a–c). By dividing SOC into POC and MAOC, however, we observed that Al_O + [1/2]Fe_O are associated with increasing levels of MAOC in both low pH and high pH soils, and that Ca_{ex} + Mg_{ex} are associated with increasing MAOC even in low pH soils (Fig 3, SI Table 10).

Although this study is limited to agricultural soils, we speculate that if the MCI proposed here were investigated in a global dataset in which SOC were fractionated into POC and MAOC, the MCI may similarly predict MAOC storage, and we present this hypothesis as an important topic of future work. Fractionating SOC gains importance in non-agricultural soils because non-agricultural soils store a greater proportion of SOC as POC (Lugato et al. 2021), and the effect of soil physicochemical controls on MAOC may be obscured by this abundance of POC.). In the global dataset of Rasmussen et al. (2018), which contained grassland and forest soils, POC may have comprised a greater proportion of SOC in extremes of water balance (Fig 5), where microbial decomposition may be limited (Cotrufo et al. 2021). In arid environments, Fe_O and Al_O may poorly correlate to SOC (Rasmussen et al., 2018) due to the prevalence of Ca_{ex} and the presence of POC, which was not related to Ca_{ex} in this study (SI Table 9). In contrast, in humid environments, Fe_O and Al_O may be related to total SOC (Rasmussen et al., 2018) due to both their prevalence and to their moderate contribution to POC stabilization (Fig 2). While the soils in this study

are a continental rather than global dataset, by fractionating SOC and studying a range of soil pH and physicochemical properties we identify the efficacy of an MCI across agricultural soils. Our data do not support the concept of a pH threshold in which a single feature of the soil matrix begins to stabilize SOC, and instead suggest that a milieu of soil compounds, differing in abundance, can operate concurrently to stabilize MAOC and that considering their unified stabilization potential offers a comprehensive view of SOC dynamics.

The utility of this MCI will vary with research aims, its generalizability across non-agricultural systems, and community reporting practices. This MCI may prove a valuable tool for parsimonious, process-based SOC modeling in that it may quantify matrix stabilization capacity beyond that of clay while avoiding the complication of representing multiple soil physicochemical properties separately. While soil pH may appear a reasonable substitute for soil texture given *pH-dependent* MAOC stabilization mechanisms, soil pH was a poor predictor of MAOC compared to the MCI (SI Table 10), likely because total matrix stabilizing agents are independent of soil pH. However, if the research aim is to understand the relative importance of soil physicochemical properties for MAOC in specific contexts, then keeping soil properties separate will enable more granular investigation than combining them in an MCI. The extent to which a similar relationship of the MCI with MAOC holds across non-agricultural ecosystems requires investigation, as do interactions of matrix stabilization with climate (Possinger et al. 2021) and stocks vs. persistence of MAOC (*sensu* Heckman et al. 2020). Finally, as the MCI of a given soil will change depending on the mean and standard deviation used to calculate z-scores, we emphasize the need for consistent reporting of means and standard deviations if MCI values are to be comparable across studies.

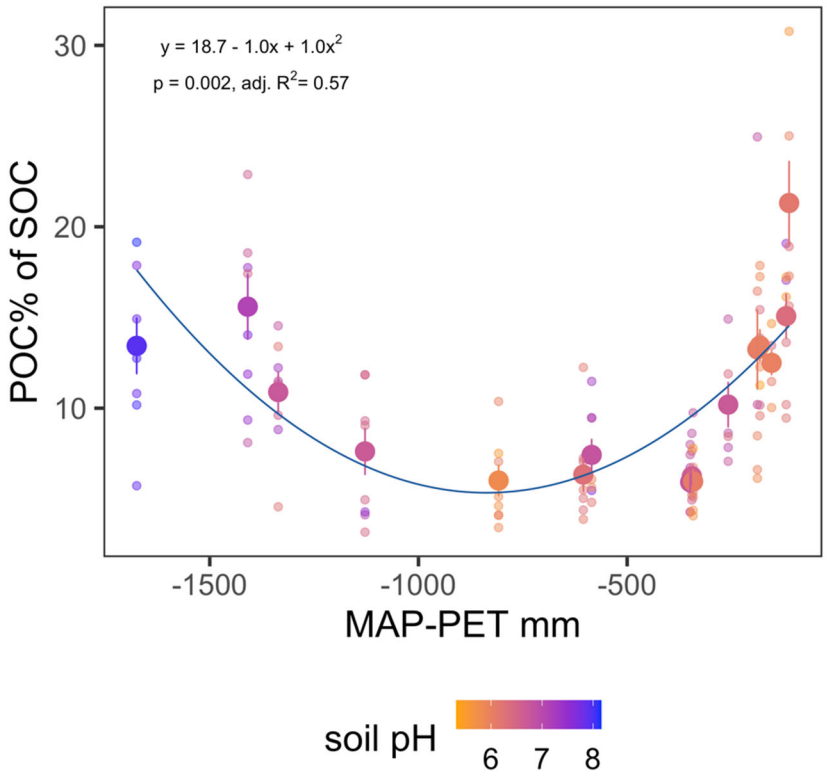

Fig. 5 Quadratic relationship between MAP-PET and particulate organic carbon (POC) as a percentage of soil organic carbon (SOC), where raw C data are in g C kg soil^{-1}. Quadratic regression was performed log transformed response; coefficients are back-transformed for presentation. Large points represent site-level averages and small points represent plots within sites (n = 124).

Direct and indirect effects of MAP-PET on POC and MAOC

To assess the direct and indirect effects of MAP-PET on soil C, we constructed two SEMs, one each for POC and MAOC (Fig 6). As potential mediators of an indirect effect of MAP-PET on POC, we used $Al_O + [1/2]Fe_O$ because it was the only factor related to POC in simple linear regression (Fig 2). Since there were many environmental properties correlated with MAOC, we used the MCI and total C inputs in the SEM, as they were the factors exhibiting the strongest relationship to MAOC in simple linear regressions (Fig 2, Fig 3). Here, we use 'direct' and 'indirect' to describe pathways elaborated in the structural equation model, acknowledging that pathways established as 'direct' in the model may nevertheless be mediated by properties not measured in this study. Structural equation modeling revealed that MAP-PET exerted only a direct effect on POC and a combination of direct and indirect effects of MAOC (Fig 6).

A direct, positive association of MAP-PET with POC was not anticipated in this study but suggests that POC pools are more sensitive to decomposition than C input rates. We predicted that higher MAP-PET would correlate with greater C inputs or greater matrix protective capacity created by $Al_O + [1/2]Fe_O$, potentially resulting in higher POC through aggregation (Wagai et al. 2020). These hypotheses were not supported by the results of the simple linear regression, which showed no relationship between C inputs and POC (Figure 4), or the results of the SEM, which showed that despite increases with MAP-PET, $Al_O + [1/2]Fe_O$ had a relatively little subsequent relationship to POC (Figure 6). Although MAP-PET likely mediates soil moisture and thereby controls rates of microbial decomposition, the extent to which increasing soil moisture in these agricultural soils could reduce microbial decomposition – and, therefore, the retention of C inputs in POC – remains an open question (Keiluweit et al. 2017). Another pathway through which MAP-PET could influence POC is that of root tissue chemistry. There is suggestive evidence that roots decrease nitrogen (N) content with increasing precipitation (Ordóñez et al. 2020), which could delay decomposition, however, this putative mechanism requires further investigation to verify.

Increasing MAP-PET had a total, positive association with MAOC, comprised primarily of indirect effects that were mediated by both increasing MCI and increasing total C inputs (Fig 5). The association of MAP-PET with the MCI was weaker than with $Al_O + [1/2]Fe_O$ but still significant, likely due to contrasting effects of MAP-PET on $Al_O + [1/2]Fe_O$ and on $Ca_{ex} + Mg_{ex}$ (Fig 1). The SEM also showed a series of positive interactions between the MCI, total C inputs, and MAOC (Fig 6). The clearest interpretation of these interactions is that both the MCI (Kleber et al. 2015; Rowley et al. 2021) and C inputs (Gulde et al. 2008) lead to higher MAOC. However, iterations of the model without an MCI – C input relationship specified were returned as poorly fit (CFI < 0.90, Hooper et al. 2008), suggesting that higher MCI also promoted crop productivity. We speculate that components of the MCI may have contributed to crop nutrient requirements: while Al is not an essential plant nutrient, Fe and Ca are, and oxalate-extractable Fe in soil can correspond to crop Fe uptake (Morris et al. 1990). As a major component of SOC, MAOC may have also positively affected crop productivity (Oldfield et al. 2018) and therefore C inputs through its benefits for soil available water holding capacity, N mineralization, and soil structure (King et al. 2020).

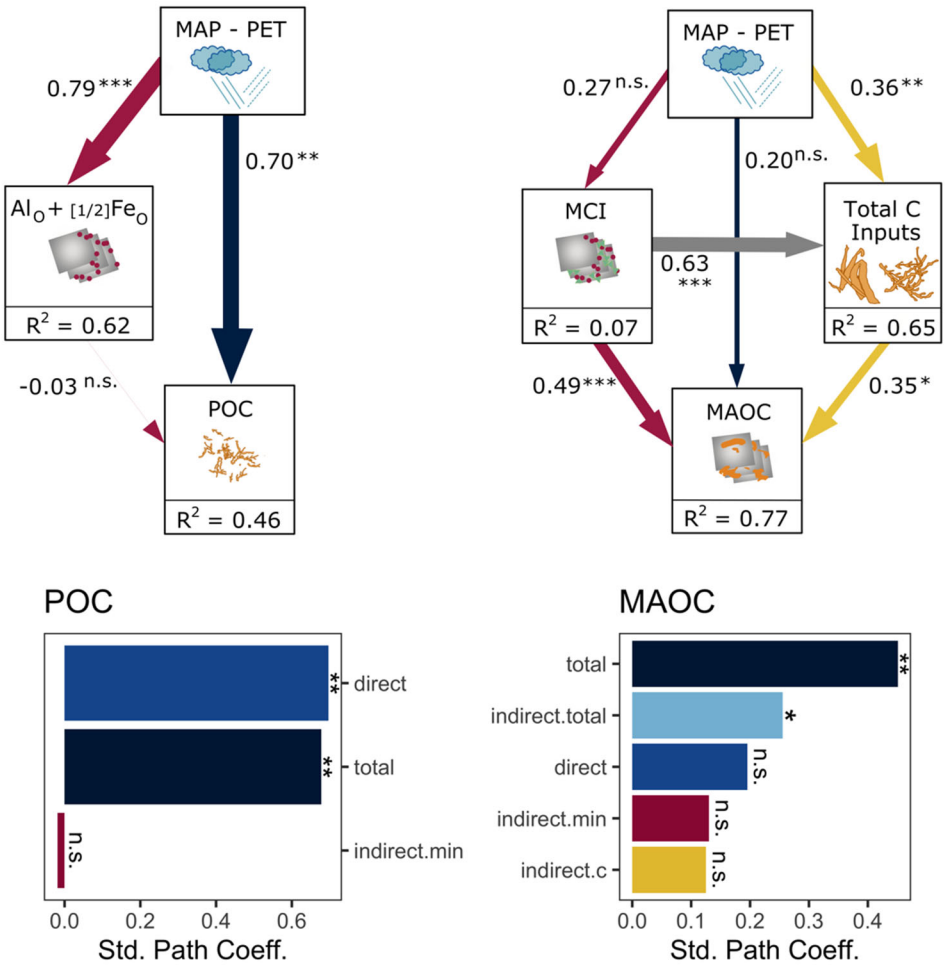

Fig. 6 Structural equation model (SEM) showing direct and indirect effects of mean annual precipitation – potential evapotranspiration (MAP-PET, mm) on particulate (POC, left) and mineral-associated (MAOC, right) organic carbon. Soils measured 0–20 cm depth across 16 agricultural sites (n = 124 plots) in the United States; site-level averages used in SEM. The SEM for POC includes Al_O + [1/2]Fe_O (g kg soil^{-1}), while the SEM for MAOC includes a matrix capacity index (MCI, unitless) and total C inputs (Mg C ha^{-1} yr^{-1}). The widths of the arrows correspond to the standardized path coefficients, which are also shown in numbers next to each arrow. R^2 values represent total proportion of variability explained by all paths. Yellow arrows and bars represent pathway from MAP-PET to C fraction as mediated by C inputs. Red arrows and bars represent pathway from MAP-PET to C fraction as mediated by soil physicochemical property. Navy arrow represents direct effect of MAP-PET on C fraction. Effects of complete paths are show in the barplot, where 'indirect.min' = effect of MAP-PET on soil C via Al_O + Fe_O or the MCI, and 'indirect.c' = effect of MAP-PET on MAOC via total C inputs. In all cases, n.s. = 'not significant'; * $p < 0.01$; ** $p < 0.05$, and ***$p < 0.01$. The SEM fit the data well, as indicated by comparative fit index (CFI > 0.9) and

root mean square error of approximation (RMSEA < 0.08) and standardized root mean square residual (SRMR < 0.08; Hooper et al. 2008). Full model output provided in SI Table 10 and SI Table 11.

Implications

Here, we show that fractionating cropland SOC into POC and MAOC allows for improved resolution of their environmental controls at the continental scale, aligning with findings from forests and grasslands. Given the strong relationship of the proposed MCI to MAOC, updating process-based soil C models to incorporate an MCI may offer a promising path for their improvement. However, the data necessary to support this effort, including MAOC, Fe_O, Al_O, Ca_{ex} and Mg_{ex} are not currently a consistent part of large-scale data products (Poggio et al. 2021). Future research will need to investigate the MCI demonstrated here for croplands across other ecosystems to understand its generalizability, as the MCI may show different relationships to MAOC in other ecosystems. Larger datasets could also allow more exhaustive weighing of different approaches for summing values of soil Fe_O, Al_O, $Ca_{ex,}$ Mg_{ex}, as well as the interacting roles of soil age, parent material, and climate in driving an MCI. Coupling investigations of an MCI with processes of C transformation, C turnover, and determinants of maximum MAOC storage, including in subsoils, will also be valuable for advancing soil C modeling. Our work shows that understanding POC dynamics requires information beyond C input quantity and soil physicochemical properties to adequately describe its variation at continental scales. Soil temperature and moisture sensors, information on C input chemistry, and/or alternative fractionation of the POC pool (i.e., by density) could allow for improved resolution of POC dynamics.

Finally, we observed a series of positive associations between crop C inputs, MAOC, and the MCI. These relationships indicate the possibility of reinforcing feedbacks between crop productivity, soil MAOC accumulation, and soil fertility, where soil fertility is measured by Ca_{ex} and Fe_O but is also associated with N supply to crops from soil organic matter. While these pathways are individually acknowledged, considering and quantifying feedbacks between these pathways over broad spatial scales and beyond croplands may allow for improved understanding of future interacting between of soils, plant growth, and climate.

Conflict of interest

462 Co-author M. Francesca Cotrufo is co-founder of Cquester Analytics, which offers soil fractionation for service. The
463 other authors have no competing interests to declare that are relevant to the content of this article.
464
465 **References**

466 Austin EE, Wickings K, Mcdaniel MD, et al (2017) Cover crop root contributions to soil carbon in a no-till corn
467 bioenergy cropping system. GCB Bioenergy 1–12. https://doi.org/10.1111/gcbb.12428
468 Bolinder MA, Janzen HH, Gregorich EG, et al (2007) An approach for estimating net primary productivity and
469 annual carbon inputs to soil for common agricultural crops in Canada. Agric Ecosyst Environ 118:29–42
470 Cambardella CA, Elliott ET (1992) Particulate Soil Organic-Matter Changes across a Grassland Cultivation
471 Sequence. Soil Sci Soc Am J 56:777–783. https://doi.org/10.2136/sssaj1992.03615995005600030017x
472 Cotrufo MF, Lavallee JM (2022) Soil organic matter formation, persistence, and functioning: A synthesis of current
473 understanding to inform its conservation and regeneration, 1st edn. Elsevier Inc.
474 Cotrufo MF, Lavallee JM, Zhang Y, et al (2021) In-N--Out: A hierarchical framework to understand and predict soil
475 carbon storage and nitrogen recycling. Glob Chang Biol 4465–4468. https://doi.org/10.1111/gcb.15782
476 Cotrufo MF, Wallenstein MD, Boot CM, et al (2013) The Microbial Efficiency-Matrix Stabilization (MEMS)
477 framework integrates plant litter decomposition with soil organic matter stabilization: Do labile plant inputs
478 form stable soil organic matter? Glob Chang Biol 19:988–995
479 Fan J, McConkey B, Wang H, Janzen H (2016) Root distribution by depth for temperate agricultural crops. F Crop
480 Res 189:68–74
481 Fick SE, Hijmans RJ (2017) WorldClim 2: new 1-km spatial resolution climate surfaces for global land areas. Int J
482 Climatol 4315:4302–4315. https://doi.org/10.1002/joc.5086
483 Gentine P, Green JK, Guérin M, et al (2019) Coupling between the terrestrial carbon and water cycles — a review.
484 Environ Res Lett
485 Georgiou K, Malhotra A, Wieder WR, et al (2021) Divergent controls of soil organic carbon between observations
486 and process-based models. Biogeochemistry 2:. https://doi.org/10.1007/s10533-021-00819-2
487 Gulde S, Chung H, Amelung W, et al (2008) Soil Carbon Saturation Controls Labile and Stable Carbon Pool
488 Dynamics. Soil Sci Soc Am J 72:605
489 Hall SJ, Ye C, Weintraub SR, Hockaday WC (2020) Molecular trade-offs in soil organic carbon composition at

continental scale. Nat Geosci 13:. https://doi.org/10.1038/s41561-020-0634-x

Harris D, Horwáth WR, van Kessel C (2001) Acid fumigation of soils to remove carbonates prior to total organic carbon or CARBON-13 isotopic analysis. Soil Sci Soc Am J 65:1853. https://doi.org/10.2136/sssaj2001.1853

Hassink J (1997) The capacity of soils to preserve organic C and N by their association with clay and silt particles. Plant Soil 191:77–87

Heckman KA, Nave LE, Bowman M, et al (2020) Divergent controls on carbon concentration and persistence between forests and grasslands of the conterminous US. Biogeochemistry 0123456789:41–56. https://doi.org/10.1007/s10533-020-00725-z

Hooper D, Coughlan J, Mullen MR (2008) Structural Equation Modelling : Guidelines for Determining Model Fit. Electron J Bus Reserach Methods 6:53–60

Jobbagy EG, Jackson RB (2000) The vertical distribution of soil organic carbon and its relation to climate and vegetation. Ecol Appl 10:423–436

Johnson JMF, Barbour NW, Weyers SL (2007) Chemical composition of crop biomass impacts its decomposition. Soil Sci Soc Am J 71:155–162

Kallenbach CM, Frey SD, Grandy AS (2016) Direct evidence for microbial-derived soil organic matter formation and its ecophysiological controls. Nat Commun 7:1–10. https://doi.org/10.1038/ncomms13630

Keiluweit M, Wanzek T, Kleber M, et al (2017) Anaerobic microsites have an unaccounted role in soil carbon stabilization. Nat Commun 1–8. https://doi.org/10.1038/s41467-017-01406-6

King AE, Ali G, Gillespie AW, Wagner-Riddle C (2020) Soil organic matter as catalyst of crop resource capture. Front Environ Sci. https://doi.org/doi: 10.3389/fenvs.2020.00050

King AE, Blesh J (2018) Crop rotations for increased soil carbon: perenniality as a guiding principle. Ecol Appl 28:249–261. https://doi.org/10.1002/eap.1648

Kleber M, Eusterhues K, Keiluweit M, et al (2015) Mineral-Organic Associations: Formation, Properties, and Relevance in Soil Environments. In: Advances in Agronomy. Elsevier Ltd, pp 1–140

Lavallee JM, Soong JL, Cotrufo MF (2020) Conceptualizing soil organic matter into particulate and mineral - associated forms to address global change in the 21st century. Glob Chang Biol 261–273. https://doi.org/10.1111/gcb.14859

Lessmann M, Ros GH, Young MD, Vries W De (2022) Global variation in soil carbon sequestration potential

through improved cropland management. 1162–1177. https://doi.org/10.1111/gcb.15954

Liang C, Schimel JP, Jastrow JD (2017) The importance of anabolism in microbial control over soil carbon storage. Nat Publ Gr 2:1–6. https://doi.org/10.1038/nmicrobiol.2017.105

Loeppert RH, Inskeep WP (1996) Iron. In: Methods of Soil Analysis, Part 3. Chemical Methods. Soil Science Society of America and American Society of Agronomy, pp 639–664

Lugato E, Lavallee JM, Haddix ML, et al (2021) Different climate sensitivity of particulate and mineral-associated soil organic matter. Nat Geosci 14:. https://doi.org/10.1038/s41561-021-00744-x

Minasny B, Malone BP, McBratney AB, et al (2017) Soil carbon 4 per mille. Geoderma 292:59–86. https://doi.org/10.1016/j.geoderma.2017.01.002

Morris DR, Loeppert RH, Moore TJ (1990) Indigenous Soil Factors Influencing Iron Chlorosis of Soybean in Calcareous Soils. Soil Sci Soc Am J. https://doi.org/10.2136/sssaj1990.03615995005400050021x

Oldfield EE, Bradford MA, Wood SA (2018) Global meta-analysis of the relationship between soil organic matter and crop yields. SOIL 5:15–32. https://doi.org/10.5194/soil-2018-21

Ordóñez RA, Archontoulis S V, Martinez-feria R, et al (2020) Root to shoot and carbon to nitrogen ratios of maize and soybean crops in the US Midwest. Eur J Agron 120:126130. https://doi.org/10.1016/j.eja.2020.126130

Poeplau C, Don A, Six J, et al (2018) Isolating organic carbon fractions with varying turnover rates in temperate agricultural soils – A comprehensive method comparison. Soil Biol Biochem 125:10–26. https://doi.org/10.1016/j.soilbio.2018.06.025

Poggio L, Sousa LM De, Batjes NH, et al (2021) SoilGrids 2.0 : producing soil information for the globe with quantified spatial uncertainty. SOIL 217–240

Possinger AR, Weiglein TL, Bowman MM, et al (2021) Climate Effects on Subsoil Carbon Loss Mediated by Soil Chemistry. Environ Sci Technol. https://doi.org/10.1021/acs.est.1c04909

Rasmussen C, Heckman K, Wieder WR, et al (2018) Beyond clay: towards an improved set of variables for predicting soil organic matter content. Biogeochemistry. https://doi.org/10.1007/s10533-018-0424-3

Rowley MC, Grand S, Verrecchia EP (2018) Calcium-mediated stabilisation of soil organic carbon. Biogeochemistry 49:27–49. https://doi.org/10.1007/s10533-017-0410-1

Rowley MC, Grand S, Verrecchia EP, Spangenberg JE (2021) Evidence linking calcium to increased organo-mineral association in soils. Biogeochemistry 153:223–241. https://doi.org/10.1007/s10533-021-00779-7

Six J, Conant RT, Paul EA, Paustian K (2002) Stabilization mechanisms of soil organic matter: Implications for C-saturation of soils. Plant Soil 241:155–176

Slessarev EW, Lin Y, Bingham NL, et al (2016) Water balance creates a threshold in soil pH at the global scale. Nat Publ Gr 540:567–569. https://doi.org/10.1038/nature20139

Thomas GW (1982) Exchangeable Cations. In: Methods of Soil Analysis, Part 2. pp 159–165

Trabucco A, Zomer RJ (2018) Global Aridity Index and Potential Evapo-Transpiration (ET0) Climate Database v2. CGIAR Consort Spat Inf

von Fromm SF, Hoyt AM, Lange M, et al (2021) Continental-scale controls on soil organic carbon across sub-Saharan Africa. SOIL 7:305–332. https://doi.org/https://doi.org/10.5194/soil-7-305-2021

von Lützow M, Kögel-Knabner I, Ekschmitt K, et al (2007) SOM fractionation methods: Relevance to functional pools and to stabilization mechanisms. Soil Biol Biochem 39:2183–2207

Wagai R, Kajiura M, Asano M (2020) Iron and aluminum association with microbially processed organic matter via meso-density aggregate formation across soils: organo-metallic glue hypothesis. SOIL 597–627

Wiesmeier M, Urbanski L, Hobley E, et al (2019) Soil organic carbon storage as a key function of soils - A review of drivers and indicators at various scales. Geoderma 333:149–162. https://doi.org/10.1016/j.geoderma.2018.07.026

Yu W, Huang W, Weintraub-leff SR, Hall SJ (2022) Where and why do particulate organic matter (POM) and mineral-associated organic matter (MAOM) differ among diverse soils ? Soil Biol Biochem 172:108756. https://doi.org/10.1016/j.soilbio.2022.108756

Zhang D, Hui D, Luo Y, Zhou G (2008) Rates of litter decomposition in terrestrial ecosystems : global patterns and controlling factors. J Plant Ecol 1:85–93. https://doi.org/10.1093/jpe/rtn002

Zhang Y, Lavallee JM, Robertson AD, et al (2021) Simulating measurable ecosystem carbon and nitrogen dynamics with the mechanistically defined MEMS 2.0 model. Biogeosciences 3147–3171

Zhou G, Xu S, Ciais P, et al (2019) Climate and litter C/N ratio constrain soil organic carbon accumulation. Natl Sci Rev. https://doi.org/10.1093/nsr/nwz045